

Interband Tunneling in InAs/AlGaSb Heterostructures: Devices for Low-Power Logic and THz Applications

Patrick Fay, Yeqing Lu, Guangle Zhou, Tim Vasen, Yi Xie, Md. Itrat Bin Shams, Ze Zhang, Huili (Grace) Xing, and Alan Seabaugh

*Department of Electrical Engineering, Univ. of Notre Dame, USA
pfay@nd.edu*

Continued advances in electronics require simultaneous increases in integration and reduction in power dissipation, while also improving performance and adding additional functionality such as sensing capabilities. With conventional silicon device scaling facing fundamental limitations, novel approaches are becoming increasingly attractive. Heterostructures in the InAs/AlGaSb material system in particular offer advantages to address these challenges. The high electron mobility of InAs, in combination with the tunability of the band offsets between AlGaSb and InAs from staggered to broken through control of the Al mole fraction, offers a rich design space for exploring promising device concepts. In this talk, two devices that leverage these unique material properties are presented. For low-power logic applications, interband tunneling field-effect transistors (TFETs) in this material system have significant advantages at low supply voltages [1,2], while at frequencies in the millimeter-wave and THz regime, InAs/AlGaSb interband tunnel diode detectors offer unprecedented sensitivity and low noise performance [3].

For TFETs, the fundamental advantage that interband tunneling provides derives from the energy filtering due to the band edges' truncation of the Fermi tails in the conduction and valence bands. Fig. 1 shows a simplified structure and band diagrams for the on- and off-state conditions for an InAs/AlGaSb vertical TFET [4]. Numerical simulations of this device indicate that subthreshold slopes approaching 7 mV/decade are possible, but to achieve this requires careful engineering of both the tunnel junction as well as the geometric electrostatics of the device [4]. This device architecture has been demonstrated experimentally; the structure and electrical characteristics are shown in Figs. 2 and 3, respectively [1]. A high drain current density of 180 $\mu\text{A}/\mu\text{m}$ was obtained at $V_{\text{DS}}=0.5$ V, indicating the potential of these devices for operation at supply voltages below that required for operation of conventional CMOS. To explore the impact of TFETs on circuit performance, physics-based simulation of logic circuits has been performed using Synopsys TCAD. Fig. 4 shows the resulting intrinsic delay, switching energy, and energy-delay product for an InAs/AlGaSb TFET-based inverter as a function of power supply voltage [2]. As tabulated in Fig. 4, at $V_{\text{DD}}=0.3$ V, TFETs offer a substantial switching energy and energy-delay product advantage over both low-power CMOS and III-V/Ge channel CMOS [5]. These results highlight the potential benefits of these devices for future-generation logic circuits.

Sensing and detection is another arena in which the use of interband tunneling improves device performance. As with TFETs, the energy filtering in InAs/AlSb/GaSb interband heterostructure diodes results in more abrupt rectification than is possible with thermionic devices such as Schottky diodes. For high-frequency square-law detection, these more strongly nonlinear current-voltage characteristics lead to increased sensitivity. Fig. 5 shows the room-temperature measured characteristics of a heterostructure detector with curvature ($\gamma = (\partial^2 I / \partial V^2) / (\partial I / \partial V)$) of 47 V^{-1} (vs. a theoretical maximum of $\gamma=q/kT=38.5$ V^{-1} for a Schottky diode) [3]. These improvements in curvature (and thus sensitivity) also improve noise equivalent power, since in the absence of external bias the devices have extremely low 1/f noise [3]. Device modeling based on self-consistent Poisson/Schrodinger simulations coupled to transfer-matrix calculations for tunneling currents (including the effects of conduction band nonparabolicity) indicate that significant further increases in sensitivity can be expected with additional device engineering, while simultaneously reducing the capacitance (for increased frequency of operation) [6]. Recent experimental results indicate an intrinsic cut-off frequency for these devices exceeds 8 THz [7], with extrinsic cutoff frequencies for antenna-coupled detectors experimentally demonstrated above 900 GHz [8].

This work was supported in part by the Semiconductor Research Corporation's Nanoelectronics Research Initiative and the National Institute of Standards and Technology through the Midwest Institute of Nanoelectronics Discovery (MIND), and by the National Science Foundation.

References

[1] G. Zhou et al., "Novel gate-recessed vertical InAs/GaSb TFETs with record high I_{ON} of 180 $\mu\text{A}/\mu\text{m}$ at $V_{DS}=0.5\text{ V}$ ", *Proc. International Electron Devices Meeting*, pp. 32.6.1, 2012.
 [2] P. Fay et al., "III-V Tunnel FETs for Energy Efficient Logic," *Proc. Workshop on Compound Semiconductor Devices and Integrated Circuits in Europe*, p. 141-144, 2013.
 [3] Z. Zhang et al., "Sub-Micron Area Heterojunction Backward Diode Millimeter-Wave Detectors with 0.18 $\text{pW}/\text{Hz}^{1/2}$ Noise Equivalent Power," *IEEE Microwave and Wireless Components Lett.*, vol. 21, p. 267, 2011.
 [4] Y. Lu et al., "Performance of AlGaSb/InAs TFETs with gate electric field and tunneling direction aligned," *IEEE Electron Device Lett.*, vol. 33, p. 655, 2012.
 [5] International Technology Roadmap for Semiconductors, (2011).
 [6] Md. Itrat Bin Shams et al., "An accurate interband tunneling model for InAs/GaSb heterostructure devices," *Physica Status Solidi C*, vol. 10, p. 740, 2013.
 [7] P. Fay et al., "High performance heterostructure backward diode detectors," *Proc. SPIE*, vol. 8031, p. 80310B, 2011.
 [8] G. Trichopoulos et al., "A Broadband Focal Plan Array Camera for Real-time THz Imaging Applications," *IEEE Trans. on Antennas and Propagation*, vol. 61, pp. 1733-1740, 2013.

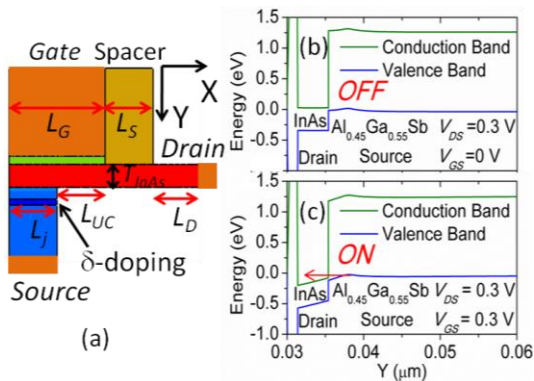


Fig. 1. (a) Schematic cross-section of vertical TFET device; (b) band diagram in the off-state, (c) band diagram in the on-state [4].

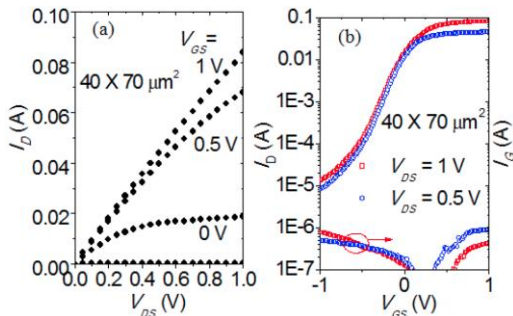


Fig. 3. Measured common-source characteristics for vertical InAs/GaSb TFET [1].

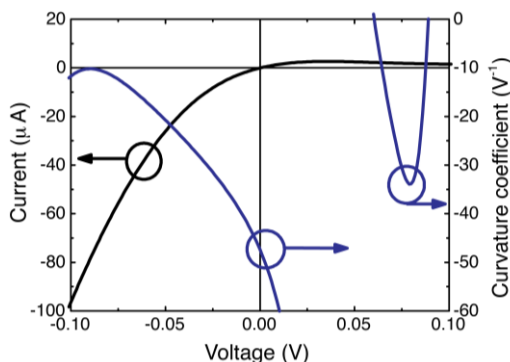


Fig. 5. Measured I-V and curvature for InAs/AlSb/AlGaSb heterostructure backward diode with record curvature of 47 V^{-1} [3].

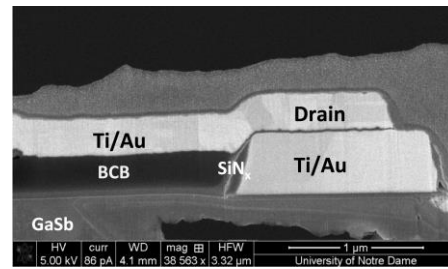


Fig. 2. Cross-section of fabricated vertical InAs/GaSb heterostructure TFET [1].

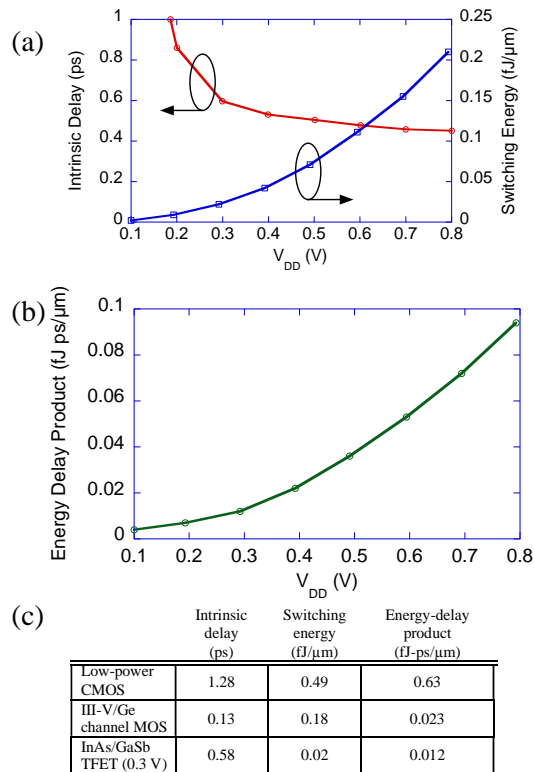


Fig. 4. (a) Simulated delay and switching energy as a function of supply voltage; (b) energy-delay product vs. supply voltage for an InAs/GaSb TFET logic inverter; (c) comparison of ITRS CMOS projections vs. InAs/GaSb TFET logic performance [2,5].